Inorganic Chemistry
Article

Inorg. Chem. **2009**, *48*, 9767–9778 **9767**
DOI: 10.1021/ic901340w

Reactions of the Unsaturated Complex $[Mo_2(\eta^5\text{-}C_5H_5)_2(\mu\text{-}PEt_2)_2(CO)_2]$ with $[Au(PR_3)]^+$ Cations: Kinetic Preference of the Mo−P Bonds as the Site of Attack of the Gold(I) Electrophile

M. Angeles Alvarez, M. Esther García, Daniel García-Vivó, M. Eugenia Martínez, and Miguel A. Ruiz*

Departamento de Química Orgánica e Inorgánica/IUQOEM, Universidad de Oviedo, E-33071 Oviedo, Spain

Received July 10, 2009

The title complex reacts with $[Au(PR_3)]^+$ cations (PF_6^- salts, R=*p*-tol, Me) in dichloromethane solutions to give first the corresponding agostic-like products $[AuMo_2Cp_2(\mu\text{-}PEt_2)(\mu_3\text{-}PEt_2)(CO)_2(PR_3)]PF_6$, which then partially rearrange to reach an equilibrium with the hydride-like isomers $[AuMo_2Cp_2(\mu\text{-}PEt_2)_2(CO)_2(PR_3)]PF_6$, the latter being characterized through an X-ray study (R=*p*-tol, Mo−Mo=2.8244(2) Å). These unsaturated complexes react smoothly with CO (1 atm) to give the corresponding electron-precise derivatives $[AuMo_2Cp_2(\mu\text{-}PEt_2)_2(CO)_3(PR_3)]^+$ (Mo−Mo = 3.0438(6) Å when R=Me), this implying the rearrangement of the μ_3-PEt_2 ligand to a more common μ_2-coordination mode. Density functional theory (DFT) calculations on the dimolybdenum complexes $[Mo_2Cp_2(\mu\text{-}PR_2)_2(CO)_2]$ (R=Cy, Et) reveal the presence of a framework M−P bonding orbital high in energy and with the right shape to act as a donor to H^+ and $[Au(PR_3)]^+$ cations, thus explaining the formation of agostic and agostic-like products respectively in these reactions. The unusually high energy of this donor orbital can be related to the close approach of the metal centers in these unsaturated molecules. The carbyne complex $[Mo_2Cp_2(\mu\text{-}COMe)(\mu\text{-}PCy_2)(CO)_2]$ reacts with $[Au\{P(p\text{-}tol)_3\}]^+$ to give the tricarbonyl $[AuMo_2Cp_2(\mu\text{-}COMe)(\mu\text{-}PCy_2)(CO)_3\{P(p\text{-}tol)_3\}]^+$ (Mo−Mo=2.986(1) Å), a process most likely initiated by the binding of the gold cation to one of the Mo−P bonds in the carbyne complex.

Introduction

Recently we reported a comprehensive study on the protonation reactions of the unsaturated complexes $[M_2Cp_2(\mu\text{-}PR_2)(\mu\text{-}PR'_2)(CO)_2]$ (M = Mo, W; R, R′ = Cy, Et, Ph), aimed initially to the synthesis of unsaturated, hydride-bridged binuclear cations.[1] However, we found that these reactions were more complex than suspected since they never involved the protonation of the metal−metal bond as the first step. Instead, we were able to prove that the protonation of these substrates at low temperature involve the initial H^+ attack at either a single metal site, to give a terminal hydride ligand (preferred route for tungsten complexes), or at a metal−phosphorus bond to give an agostic-type $\mu\text{-}\kappa^2\text{-}HPR_2$ bridging phosphine ligand (preferred route for molybdenum complexes when R = Cy, Et). The terminal hydride complexes $[M_2Cp_2(H)(\mu\text{-}PR_2)(\mu\text{-}PR'_2)(CO)_2]^+$ are thermally unstable, and at room temperature they rearrange to give the corresponding hydride-bridged isomers $[M_2Cp_2(\mu\text{-}H)(\mu\text{-}PR_2)(\mu\text{-}PR'_2)(CO)_2]^+$. In contrast, the phosphine-bridged complexes $[Mo_2Cp_2(\mu\text{-}\kappa^2\text{-}HPR_2)(\mu\text{-}PR'_2)(CO)_2]^+$ only rearrange partially at room temperature, to reach an equilibrium with the corresponding hydride-bridged tautomers $[Mo_2Cp_2(\mu\text{-}H)(\mu\text{-}PR_2)(\mu\text{-}PR'_2)(CO)_2]^+$ (Scheme 1).[1] Phosphine-bridged complexes exhibiting agostic-type M−H−P interactions are very rare species, and only a few palladium complexes of type $[Pd_2(\mu\text{-}PR_2)(\mu\text{-}\kappa^2\text{-}HPR_2)L_2]^+$ (R = ^{t}Bu, Cy; L = phosphine ligand)[2] and the platinum complex $[Pt_2(\mu\text{-}P^tBu_2)(\mu\text{-}\kappa^2\text{-}PH^tBu_2)(C_2H_4)_2]^+$ have been described so far.[3] Further interest in these species stems from the fact that the coordination of the P−H bond of a phosphine ligand to a metal atom weakens that bond and is expected to result in specific reactivity. It also represents an intermediate step in the oxidative addition of P−H bonds of primary and secondary phosphines to unsaturated dimetal centers.[4,5]

*To whom correspondence should be addressed. E-mail: mara@uniovi.es.

(1) Alvarez, M. A.; García, M. E.; Martínez, M. E.; Ramos, A.; Ruiz, M. A.; Sáez, D. *Inorg. Chem.* **2006**, *45*, 6965.

(2) (a) Albinati, A.; Lianza, F.; Pasquali, M.; Sommovigo, M.; Leoni, P.; Pregosin, P. S.; Rüeger, H. *Inorg. Chem.* **1991**, *30*, 25. (b) Leoni, P.; Pasquali, M.; Sommovigo, M.; Laschi, F.; Zanello, P.; Albinati, A.; Lianza, F.; Pregosin, P. S.; Rüeger, H. *Organometallics* **1993**, *12*, 1702. (c) Leoni, P.; Pasquali, M.; Sommovigo, M.; Albinati, A.; Lianza, F.; Pregosin, P. S.; Rüeger, H. *Organometallics* **1994**, *13*, 4017. (d) Leoni, P.; Vichi, E.; Leonci, S.; Pasquali, M.; Chiarentin, E.; Albinati, A. *Organometallics* **2000**, *19*, 3062.

(3) Leoni, P.; Marchetti, F.; Marchetti, L.; Passarelli, V. *Chem. Commun.* **2004**, 2346.

(4) (a) Alvarez, M. A.; Anaya, Y.; García, M. E.; Riera, V.; Ruiz, M. A. *Organometallics* **2004**, *23*, 433. (b) Alvarez, C. M.; Riera, V.; Ruiz, M. A.; Connelly, N. G. *Organometallics* **2004**, *23*, 4750.

(5) García, M. E.; Riera, V.; Ruiz, M. A.; Rueda, M. T.; Sáez, D. *Organometallics* **2002**, *21*, 5515.

Published on Web 09/18/2009

Scheme 1. Protonation Reactions of the Unsaturated Complexes $[M_2Cp_2(\mu\text{-}PR_2)(\mu\text{-}PR'_2)(CO)_2]$[a]

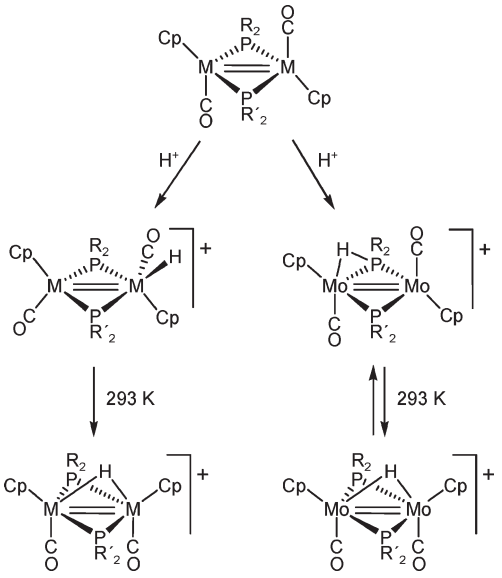

[a] Adapted from reference 1; M = Mo, W.

Because of the isolobal analogy relating a proton with the gold(I) cations $[Au(PR_3)]^+$,[6] it might be conceived that if a proton can attack an M−P bond in a PR_2-bridged substrate to give a κ^2-HPR_2 bridged derivative, then the reaction of such substrate with a cation of the type $[Au(PR_3)]^+$ might analogously involve the electrophilic attack of the gold(I) cation to one of its M−P bonds to yield an heterometallic derivative having the PR_2 ligand bridging three metal atoms by virtue of the new tricentric MPAu interaction being established (Scheme 2). Indeed, there is one precedent of this sort of reaction, namely, the reaction between the diplatinum complex $[Pt_2(\mu\text{-}PPh_2)_2(PPh_3)_2]$ and $[Au(PPh_3)]PF_6$ to give the tetrametallic derivative $[Au_2Pt_2(\mu_3\text{-}PPh_2)_2(PPh_3)_4](PF_6)_2$, although the incoming $Au(PPh_3)^+$ cations in that case seem to be more strongly bound to the platinum atoms, according to the corresponding X-ray diffraction data.[7] Actually, the formation of this tetrametallic cation was cleverly used to predict the possibility of preparing κ^2-HPR_2 bridged complexes through protonation reactions, a method materialized a few years later on the mentioned dipalladium complexes. With these precedents at hand we decided to examine the reactions of the unsaturated complexes $[M_2Cp_2(\mu\text{-}PR_2)(\mu\text{-}PR'_2)(CO)_2]$ with $[Au(PR_3)]^+$ cations as a possible systematic route to heterometallic derivatives having PR_2 ligands bridging three metal atoms. Complexes having μ_3-PR_2 bridges are still rare species, and only a handful of these polynuclear species have been reported so far, most of them involving Pt_3 and Ru_3 centers.[8,9] By following our mentioned study on protonation reactions, we chose those substrates leading to

Scheme 2

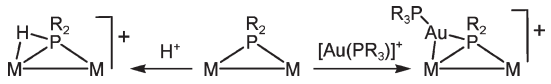

the highest proportion of agostic κ^2-HPR_2 derivatives, these being the dimolybdenum complexes $[Mo_2Cp_2(\mu\text{-}PR_2)_2(CO)_2]$ (R = Cy, Et).[1] Unfortunately the dicyclohexylphosphide complex was found to be inert toward different gold(I) cations, perhaps because of its great steric crowding. In this paper we report our results on the reactions of the diethylphosphide complex with different $[Au(PR_3)]^+$ cations. As it will be discussed, these reactions proceed analogously to the protonation reactions, first involving the electrophilic attack of the gold(I) cation to one of the Mo−P bonds, to give a μ_3-PEt_2 derivative which then rearranges to reach an equilibrium with the tautomer having the gold(I) cation bridging the Mo−Mo bond, this being itself unprecedented. We have also carried out Density Functional Theory (DFT) calculations on the complexes $[Mo_2Cp_2(\mu\text{-}PR_2)_2(CO)_2]$ (R = Cy, Et) to better understand the reactions of these substrates with gold(I) cations and with protons. Finally, we also report our results on related reactions using the methoxycarbyne complex $[Mo_2Cp_2(\mu\text{-}COMe)(\mu\text{-}PCy_2)(CO)_2]$[10] as starting substrate, these suggesting the occurrence of a similar pathway for the electrophilic attack of the gold(I) cation to the Mo−P (rather than Mo−C) bond of this unsaturated complex.

Results and Discussion

Reactions of the Complex $[Mo_2Cp_2(\mu\text{-}PEt_2)_2(CO)_2]$ with Cations of Type $[Au(PR_3)]^+$. The title compound reacts smoothly at room temperature or even at 273 K with different $[Au(PR_3)]^+$ cations, as generated "in situ" from the corresponding $[AuCl(PR_3)]$ complexes and $TlPF_6$ in dichloromethane solution, to give products of nature and stability strongly dependent on the gold-bound phosphine being present. When R = *p*-tol or Me, the above reaction gives an equilibrium mixture of the corresponding agostic-like products $[AuMo_2Cp_2(\mu\text{-}PEt_2)(\mu_3\text{-}PEt_2)(CO)_2(PR_3)]PF_6$ [R = *p*-tol (**1a**), Me (**1b**)] and the corresponding hydride-like isomers $[AuMo_2Cp_2(\mu\text{-}PEt_2)_2(CO)_2(PR_3)]PF_6$ (**2a**,**b**), as well as some side-products arising from the decomposition of the gold(I) cations (Scheme 3). When R = ^{i}Pr, however, the above reaction led to a complex mixture of products that could not be properly purified or characterized, although species of the types **1** and **2** are probably present in these mixtures.

The equilibrium ratio between the isomers **1** and **2** is dependent on the gold-bound phosphine, with the ratio **1**/**2** being about 1:3 when R = *p*-tol and 1:1 when R = Me. This is somehow consistent with our previous studies on the protonation reactions of the complexes $[Mo_2Cp_2(\mu\text{-}PR_2)(\mu\text{-}PR'_2)(CO)_2]$, these showing that the agostic κ^2-HPR_2 derivatives are favored over their hydride-bridged tautomers for the better donor and smaller substituents on the PR_2 bridges.[1] Also in parallel with these protonation reactions, we have found (through IR monitoring of the corresponding reaction mixtures) that the attack of

(6) Evans, D. G.; Mingos, D. M. P. *J. Organomet. Chem.* **1982**, *232*, 171.
(7) Bender, R.; Braunstein, P.; Dedieu, A.; Dusausoy, Y. *Angew. Chem., Int. Ed. Engl.* **1989**, *7*, 923.
(8) Mastrorilli, P. *Eur. J. Inorg. Chem.* **2008**, 4835.
(9) For some recent work on this subject see: (a) Chaouche, N.; Forniés, J.; Fortuño, C.; Kribii, A.; Martín, A. *J. Organomet. Chem.* **2007**, *692*, 1168. (b) Díez, A.; Forniés, J.; García, A.; Lalinde, E.; Moreno, M. T. *Inorg. Chem. Commun.* **2006**, *9*, 255. (c) Alonso, E.; Forniés, J.; Fortuño, C.; Martín, A.; Orpen, A. G. *Organometallics* **2003**, *22*, 2723, and references therein. (d) Low, P. J.; Udachin, K. A.; Carty, A. J. *J. Cluster Sci.* **2004**, *15*, 277. (e) Zhong, X.; Ang, S. G.; Ang, H. G. *J. Organomet. Chem.* **2004**, *689*, 361.
(10) García, M. E.; García-Vivó, D.; Ruiz, M. A.; Alvarez, S.; Aullón, G. *Organometallics* **2007**, *26*, 5912.

Scheme 3

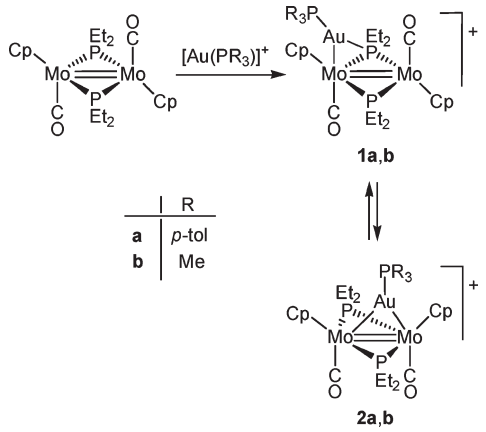

the gold(I) cation first gives the agostic-like compounds **1**, these partially rearranging afterward to give the hydride-like tautomers **2**. We note that such isomerization requires substantial rearrangement, since the CpMo(CO) fragments in the isomers **2** must adopt a *cisoid* conformation, as opposed to the *transoid* conformation in the isomers **1**. Yet, the process is moderately fast at room temperature. Thus, the ^{1}H and ^{31}P NMR spectra recorded on a solution obtained by dissolving single crystals of the isomer **2a** (from the same crop used in the X-ray diffraction study of the complex) in CD_2Cl_2, reveal that the equilibrium between isomers **2a** and **1a** is reached in about 10 min at room temperature.

The equilibrium between the isomers **1** and **2** involves the reversible migration of the corresponding $[Au(PR_3)]^+$ cation between the M−P and the M−M bonds of a M_2P triangle in a phosphide-bridged complex. To our knowledge this dynamic behavior has no precedent in the literature. However, since this rearrangement also involves a dramatic change in the relative conformation of the MoCp(CO) fragments, we will make no attempt to provide a simple interpretation of the observed trends.

Structural Characterization of Compounds 1 and 2. The structure of compound **2a** has been determined through an X-ray diffraction study. A view of the cation is shown in the Figure 1, while the most relevant bond distances and angles are collected in the Table 1. The cation can be viewed as made up from two MoCp(CO) fragments arranged in a cisoid conformation and symmetrically bridged by two diethylphosphide ligands and by a gold-phosphine fragment. The carbonyl ligands, which are almost parallel to each other and are placed *trans* to the Au atom, lie in Mo_2Au plane, which is in turn almost perpendicular to the average Mo_2P_2 plane defined by the molybdenum and P(phosphide) atoms. As expected, the Mo−Au lengths of about 2.82 Å are longer than those of conventional (bicentric) Mo−Au bonds (for instance, ca. 2.71 Å in $[AuMoCp(CO)_3(PPh_3)]$),[11] and they can be considered as sensible figures for a 3-center 2-electron interaction. Unfortunately there are not many Mo_2Au clusters structurally characterized to be used for comparative purposes, but we note that the Mo−Au lengths

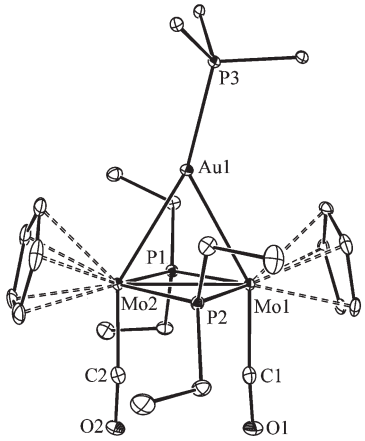

Figure 1. ORTEP diagram (30% probability) of the cation in compound **2a**, with H atoms and *p*-tol groups (except the C^1 atoms) omitted for clarity.

Table 1. Selected Bond Lengths (Å) and Angles (deg) for Compound **2a**

Mo(1)−Mo(2)	2.8244(2)	Mo(1)−Au(1)−Mo(2)	60.2(1)
Mo(1)−Au(1)	2.8222(2)	Mo(1)−P(1)−Mo(2)	71.8(1)
Mo(2)−Au(1)	2.8110(2)	Mo(1)−P(2)−Mo(2)	71.8(1)
Mo(1)−P(1)	2.4060(5)	Mo(1)−C(1)−O(1)	175.8(2)
Mo(1)−P(2)	2.4069(5)	Mo(2)−C(2)−O(2)	176.7(2)
Mo(2)−P(1)	2.4125(5)	Mo(1)−Mo(2)−C(2)	88.4(1)
Mo(2)−P(2)	2.4088(5)	Mo(2)−Mo(1)−C(1)	91.3(1)
Mo(1)−C(1)	1.966(2)	P(1)−Mo(1)−C(1)	91.7(1)
Mo(2)−C(2)	1.976(2)	P(1)−Mo(2)−C(2)	87.1(1)
C(1)−O(1)	1.155(3)	P(2)−Mo(1)−C(1)	87.8(1)
C(2)−O(2)	1.153(3)	P(2)−Mo(2)−C(2)	89.1(1)
		Au(1)−Mo(1)−C(1)	150.8(1)
		Au(1)−Mo(2)−C(2)	148.5(1)
		Mo(1)−Au(1)−P(3)	137.7(1)
		Mo(2)−Au(1)−P(3)	161.0(1)

in **2a** are not far from the average figure of the Mo−Au lengths measured in the neutral compound $[AuMo_2Cp_2(\mu\text{-}PPh_2)(CO)_4(PPh_3)]$ (Mo−Au = 2.785(1) and 2.975(1) Å).[12] Finally, we note that the Mo−Mo length of 2.8244(2) Å in **2a** is about 0.06 Å longer than the intermetallic separation in the isoelectronic and isolobal-related cation $[W_2Cp_2(\mu\text{-}H)(\mu\text{-}PPh_2)_2(CO)_2]BF_4$ (2.7589(8) Å).[1] This lengthening in the intermetallic separation when replacing the small hydrogen atom by the isoelectronic $[Au(PR_3)]^+$ cation is not unexpected, and it can be mainly ascribed to the steric demands imposed by the relatively bulky gold cation. We note that comparable elongation effects can be appreciated in other isoelectronic pairs formally involving multiple metal−metal bonds, such as the 30-electron complexes $[Mo_2Cp_2(\mu\text{-}H)(\mu\text{-}PCy_2)(CO)_2]$ (2.528(2) Å)[13] and $[Mo_2Cp_2(\mu\text{-}SnPh_3)(\mu\text{-}PCy_2)(CO)_2]$ (2.5743(7) Å),[14] or the 32-electron complexes $[Mn_2(\mu\text{-}H)_2(CO)_6(\mu\text{-}Ph_2PCH_2PPh_2)]$ (2.6999(2) Å)[15] and $[Mn_2\{\mu\text{-}Au(PPh_3)\}(\mu\text{-}H)(CO)_6\{\mu\text{-}(EtO)_2POP(OEt)_2\}]$ (2.739(3) Å).[16]

(11) Pethe, J.; Maichle-Mössmer, C.; Strähle, J. *Z. Anorg. Allg. Chem.* **1997**, *623*, 1413.

(12) Hartung, H.; Walter, B.; Baumeister, U.; Bottcher, H.-C.; Krung, A.; Rosche, F.; Jones, P. G. *Polyhedron* **1992**, *11*, 1563.

(13) Alvarez, C. M.; Alvarez, M. A.; García, M. E.; Ramos, A.; Ruiz, M. A.; Lanfranchi, M. *Organometallics* **2005**, *24*, 7.

(14) Alvarez, M. A.; García, M. E.; Ramos, A.; Ruiz, M. A. *Organometallics* **2006**, *25*, 5374.

(15) García-Alonso, F. J.; García-Sanz, M.; Riera, V.; Ruiz, M. A.; Tiripicchio, A.; Tiripicchio-Camellini, M. *Angew. Chem., Int. Ed. Engl.* **1988**, *27*, 1167.

(16) Riera, V.; Ruiz, M. A.; Tiripicchio, A.; Tiripicchio-Camellini, M. *Organometallics* **1993**, *12*, 2962.

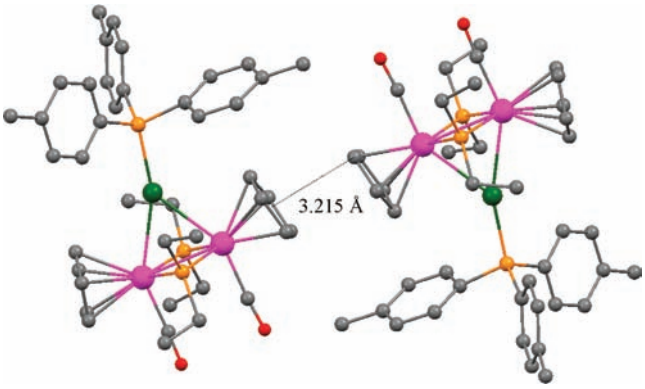

Figure 2. View of the cation−cation pairing in the lattice of compound **2a**, with H atoms and *p*-tol groups (except the C^1 atoms) omitted for clarity.

An unexpected feature in the structure of the cation in **2a** is the relatively asymmetric positioning of the gold-bound phosphine, as revealed by the substantially different Mo−Au−P(3) angles of about 138 and 161°, since there is no apparent internal reason for this asymmetry. An inspection of the packing in the lattice reveals the presence of intermolecular interactions effectively reducing the symmetry of the isolated cations, after realizing that these are arranged in centrosymmetric pairs held together by strong $\pi-\pi$ stacking interactions[17] between the adjacent Cp ligands (Figure 2). The interligand approaches (shortest C−centroid distances of ca. 3.21 Å) are significantly shorter than the interlaminar spacing in graphite (ca. 3.35 Å) in spite of unfavorable electrostatic (cation−cation) repulsions, and must therefore be taken as indicative of a particularly strong interaction.

The spectroscopic data in solution for compounds **2a**,**b** (Table 2 and Experimental Section) are consistent with the structure found for **2a** in the crystal. In the first place, their IR spectra exhibit in each case two C−O stretching bands with the pattern (strong and weak, in order of decreasing frequencies) characteristic of *cisoid* $M_2(CO)_2$ oscillators having almost parallel carbonyl ligands,[18] while their frequencies are similar to those of $[Mo_2Cp_2(\mu\text{-}H)(\mu\text{-}PEt_2)_2(CO)_2]BF_4$ (ca. 1990 cm^{-1}),[1] but displaced toward lower wavenumbers, as expected from the replacement of a hydrogen atom by the less electronegative $Au(PR_3)$ fragments. The two equivalent diethylphosphide bridges give rise to a considerably shielded ^{31}P NMR resonance at about 98 ppm, as found for the above hydride-bridged complex (61.4 ppm). This shielding effect seems to be characteristic of phosphide-bridged Mo_2 and W_2 cyclopentadienyl cations displaying flat M_2P_2 cores, as noticed previously by us,[1] and seems to be even stronger in electron-precise cations. For instance, the 34-electron complex $[Mo_2Cp_2(\mu\text{-}COMe)(\mu\text{-}PEt_2)_2(CN^tBu)_2]BF_4$ displays a ^{31}P resonance with a chemical shift as low as 47.5 ppm.[19]

The spectroscopic data in solution for compounds **1a**,**b** (Table 2 and Experimental Section) are indicative of a more asymmetric structure rendering inequivalent cyclopentadienyl groups. The carbonyl ligands seem to retain the antiparallel arrangement of the neutral starting substrate, since they give rise in each case to two C−O stretching bands of weak and strong intensities at about 1905 and 1885 cm^{-1}, respectively. This is also consistent with the fact that compounds **1** are the kinetic products in these reactions, since their formation would only require a minimum structural rearrangement of the starting complex. Besides this, the IR bands of compounds **1** have a pattern comparable to those exhibited by the related agostic-type complex $[Mo_2Cp_2(\mu\text{-}PEt_2)(\mu\text{-}\kappa^2\text{-}HPEt_2)(CO)_2]BF_4$ (1956 (m, sh), 1915 (vs) cm^{-1}),[1] but displaced toward lower wave numbers, as expected from the $H/Au(PR_3)$ formal replacement. Moreover, the diethylphosphide ligands give rise to two very differently shielded resonances (δ ca. 195 and 100 ppm), as found for the above $\mu\text{-}\kappa^2\text{-}HPEt_2$ complex (145.0 and 91.4 ppm).[1] In contrast, related isomers of the type $[M_2Cp_2(H)(\mu\text{-}PR_2)(\mu\text{-}PR'_2)(CO)_2]^+$, resulting from the incorporation of a proton to the metal site as a terminal ligand, display not so different PR_2 resonances, while the C−O stretching bands are well separated and have comparable intensities (cf. δ_P = 158.5, 152.7 ppm, and ν_{CO} = 2003 (s), 1928 (vs) cm^{-1} for the dimolybdenum complex with R = R′ = Ph).[1] We take all this as a strong indication that the $Au(PR_3)$ fragment in the complexes **1** is placed over a Mo−P bond, rather than being terminally bound to a molybdenum atom, this causing a considerable shielding on the ^{31}P nucleus of the corresponding PEt_2 group, now more properly described as a μ_3-PEt_2 ligand. Strong shielding of the PR_2 resonances have been also observed previously in several polynuclear complexes when going from μ_2 to μ_3-bridging modes.[9a,b]

Carbonylation of Compounds 1 and 2. The trimethylphosphine complexes **1b** and **2b** are thermally unstable, and they slowly decompose in solution at room temperature to give the electron-precise tricarbonyl derivative $[AuMo_2Cp_2(\mu\text{-}PEt_2)_2(CO)_3(PMe_3)]PF_6$ (**3b**) in about 40 h (Chart 1). As expected, compound **3b** can be formed more rapidly by stirring dichloromethane solutions of the compounds **1b** and **2b** under a CO atmosphere, the process being then completed in just 2 h with good yield. In a similar way, the tris(*p*-tolyl)phosphine complexes **1a** and **2a** react with CO (1 atm) in dichloromethane solution to slowly give the corresponding tricarbonyl derivative $[AuMo_2Cp_2(\mu\text{-}PEt_2)_2(CO)_3\{P(p\text{-}tol)_3\}]PF_6$ (**3a**) in good yield, the transformation being completed in about 16 h at room temperature. As it is discussed below, the formation of compounds **3** requires substantial rearrangement with respect to the unsaturated substrates **1** or **2**; therefore it is not surprising that their formation is a relatively slow process, even if the electron-precise nature of these tricarbonyl complexes makes them quite stable molecules.

The structure of compound **3b** has been established through a single-crystal X-ray diffraction study (Table 3 and Figure 3). The cation exhibits a triangular Mo_2Au metal core made up from $MoCp(CO)_2$, MoCp(CO), and $AuP(p\text{-}tol)_3$ fragments and bridged by two phosphide ligands. One of them binds asymmetrically the molybdenum atoms (Mo−P(1) = 2.402(2) and 2.458(1) Å) and is placed almost normal to the metallic plane. In contrast, the second ligand binds the monocarbonylic Mo atom

(17) Chen, X. M.; Tong, M. L. In *Frontiers in Crystal Engineering*; Tiekink, E. R. T., Vittal, J. J., Eds.; Wiley: Chichester, U. K., 2006; Chapter 10.
(18) Braterman, P. S. *Metal Carbonyl Spectra*; Academic Press: London, U. K., 1975.
(19) García, M. E.; García-Vivó, D.; Ruiz, M. A.; Herson, P. *Organometallics* **2008**, *27*, 3879.

Table 2. Selected IR[a] and NMR[b] Data for New Compounds

compound	ν(CO)[a]	δ(P)[b]/[J_{PP}]		
		μ_2-P	μ_3-P	Au-PR_3
$[AuMo_2Cp_2(\mu\text{-}PEt_2)(\mu_3\text{-}PEt_2)(CO)_2\{P(p\text{-}tol)_3\}]PF_6$ (**1a**)	1908 (w, sh), 1889 (vs)	196.1	98.4	44.5
$[AuMo_2Cp_2(\mu\text{-}PEt_2)(\mu_3\text{-}PEt_2)(CO)_2(PMe_3)]PF_6$ (**1b**)	1906 (w, sh), 1884 (vs)	193.2	99.9	11.0
$[AuMo_2Cp_2(\mu\text{-}PEt_2)_2(CO)_2\{P(p\text{-}tol)_3\}]PF_6$ (**2a**)	1967 (vs), 1928 (w)	98.2 [24]		56.3 [24]
$[AuMo_2Cp_2(\mu\text{-}PEt_2)_2(CO)_2(PMe_3)]PF_6$ (**2b**)	1963 (vs), 1943 (w)	98.9 [25]		26.2 [25]
$[AuMo_2Cp_2(\mu\text{-}PEt_2)_2(CO)_3\{P(p\text{-}tol)_3\}]PF_6$ (**3a**)	1927 (w), 1883 (vs), 1827 (m)	267.9, 193.6		43.6
$[AuMo_2Cp_2(\mu\text{-}PEt_2)_2(CO)_3(PMe_3)]PF_6$ (**3b**)	1929 (w), 1883 (vs), 1815 (m)	271.0 [14,7] 194.4 [26,7]		9.1 [26,14]
$[AuMo_2Cp_2(\mu\text{-}COMe)(\mu\text{-}PCy_2)(CO)_3\{P(p\text{-}tol)_3\}]PF_6$ (**4**)	1969 (s), 1918 (vs), 1862 (d)	286.3 [21]		34.5 [21]

[a] Recorded in dichloromethane solution, ν in cm^{-1}. [b] Recorded in CD_2Cl_2 solutions at 290 K and 121.50 MHz, δ in ppm relative to external 85% aqueous H_3PO_4 (^{31}P); J in Hz.; in addition to the resonances shown above, all compounds displayed a septet resonance at ca. −144.5 ppm (J_{PF} = 712 Hz) due to the PF_6^- anion.

Chart 1

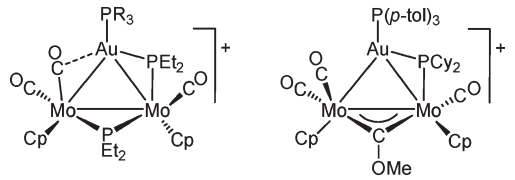

R= *p*-tol (**3a**), Me (**3b**) **4**

Table 3. Selected Bond Lengths (Å) and Angles (deg) for Compound **3b**

Mo(1)−Mo(2)	3.0437(8)	Mo(1)−Au(1)−Mo(2)	64.6(1)
Mo(1)−Au(1)	2.8382(8)	Mo(1)−P(1)−Mo(2)	77.5(1)
Mo(2)−Au(1)	2.8555(6)	Au(1)−P(2)−Mo(2)	75.5(1)
Mo(1)−P(1)	2.402(2)	Mo(1)−C(1)−O(1)	170.2(4)
Mo(2)−P(1)	2.458(1)	Mo(1)−C(2)−O(2)	160.3(5)
Mo(2)−P(2)	2.332(2)	Mo(2)−C(3)−O(3)	173.5(5)
Au(1)−P(2)	2.333(2)	Au(1)−Mo(1)−C(2)	58.7(2)
Au(1)−P(3	2.327(1)	Mo(1)−Au(1)−P(3)	130.9(1)
Mo(1)−C(1)	2.000(5)	Mo(2)−Au(1)−P(3)	163.6(1)
Mo(1)−C(2)	1.968(5)	P(1)−Mo(1)−C(1)	121.1(2)
Mo(2)−C(3)	1.930(6)	P(1)−Mo(1)−C(2)	98.4(2)
Au(1)−C(2)	2.476(5)	P(1)−Mo(2)−C(3)	68.4(2)
C(1)−O(1)	1.150(6)	P(2)−Mo(2)−C(3)	82.5(2)
C(2)−O(2)	1.165(5)	P(1)−Mo(2)−P(2)	110.1(1)
C(3)−O(3)	1.156(6)	P(2)−Au(1)−P(3)	112.9(1)

and the gold atom very tightly, as judged from the quite short interatomic lengths of about 2.33 Å. As for the carbonyl ligands, two of them are essentially terminal and are placed *trans* to each other, close to the $Mo_2P(1)$ plane. In contrast, the second carbonyl on Mo(2) is placed within the metallic plane and is clearly involved in a bent semibridging interaction with the gold atom (C(2)···Au(1) = 2.476(5) Å; Mo(1)−C(2)−O(2) = 160.3(5)°). This type of semibridging interactions are not unusual in heterometallic carbonyl clusters containing gold-phosphine fragments,[20] although it is not obvious whether they are of a truly bonding nature in all cases. For instance, comparable C····Au approaches have been found in the related carbonyl clusters $[AuMo_2Cp_2(\mu\text{-}PPh_2)(CO)_4(PPh_3)]$ (2.405(5) Å),[12] and $[Au_3Mn_2\{\mu\text{-}P(OEt)_2\}(CO)_6(PPh_3)_3]$ (2.51(2) and 2.56(2) Å).[21]

(20) Reviews: (a) Robert, D. A.; Geoffroy, G. L. In *Comprehensive Organometallic Chemistry*; Wilkinson, G., Stone, F. G. A., Abel, E. W., Eds.; Pergamon: Oxford, U.K. 1982; Vol. *6*, Chapter 40. (b) Salter, I. D. *Adv. Organomet. Chem.* **1989**, *29*, 249. (c) Mingos, D. M. P.; Watson, M. J. *Adv. Inorg. Chem.* **1992**, *39*, 327. (d) Salter, I. D. In *Comprehensive Organometallic Chemistry*, 2nd ed.; Abel, E. W., Stone, F. G. A., Wilkinson, G., Eds.; Pergamon: Oxford, U.K. 1995; Vol. *10*, Chapter 5.

(21) Liu, X. Y.; Riera, V.; Ruiz, M. A.; Tiripicchio, M.; Tiripichhio-Camellini, M. *Organometallics* **1996**, *15*, 974.

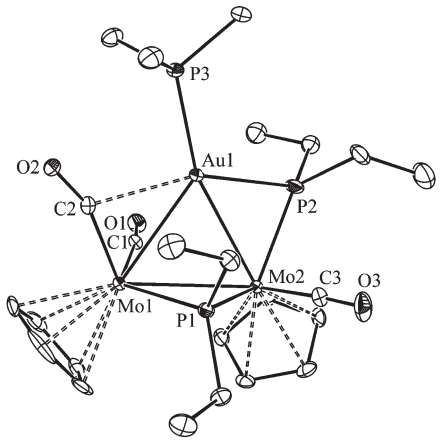

Figure 3. ORTEP diagram (30% probability) of the cation in compound **3b**, with H atoms omitted for clarity.

According to the EAN formalism, compound **3b** can be considered to be electron-precise and therefore a single Mo−Mo bond should be formulated for this cation. This is in agreement with the Mo−Mo length of 3.0437(8) Å, about 0.22 Å longer than the intermetallic separation in the unsaturated cation **2a**, although this length is still shorter than the one measured in the electron-precise trinuclear cluster $[AuMo_2Cp_2(\mu\text{-}PPh_2)(CO)_4(PPh_3)]$ (3.238(1) Å). Besides, the Mo−Au lengths of about 2.84 Å are similar to those measured for **2a** and then point to a description of the Mo−Au interaction in terms of a 3-center 2-electron bond.

The most unusual feature in the structure of **3b** concerns the coordination environment of the gold atom. Typically, single gold-phosphine fragments in heterometallic clusters are found as bridging groups over M_2 edges or M_3 faces without additional interactions.[20] In contrast, even after ignoring the semibridging interaction with the carbonyl ligand in complex **3b**, the corresponding gold-phosphine fragment is not just bound to the Mo−Mo edge, but also strongly bound to one of the phosphide ligands. We might then interpret the coordination environment around the gold atom in **3b** as one of the T-shaped type, with the three donors being the phosphine, phosphide, and the Mo−Mo bond, which is in agreement with the values of the corresponding intermetallic distances. If we label as Q the midpoint of the Mo−Mo bond, then the angles P(3)−Au(1)−Q, P(3)−Au(1)−P(2), and Q−Au(1)−P(2) are 163, 113, and 84°, respectively, with the

deviation from the regular figures of 180, 90, and 90 being easily explained as resulting from the steric repulsions between the coplanar phosphine and phosphide ligands. Alternatively, if taking into consideration the interaction with the semibridging carbonyl, then the coordination environment around the gold atom might be described as distorted square-planar, which is also unusual for a gold-(I) complex.

Spectroscopic data in solution for compounds **3a**,**b** (Table 2 and Experimental Section) are consistent with the structure found in the crystal for **3b**. These tricarbonyl complexes exhibit in each case three C−O stretching bands in the corresponding IR spectra, one of them having a rather low frequency (ca. 1820 cm^{-1}), thus suggesting the retention of a semibridging carbonyl in solution. The $^{31}P\{^1H\}$ NMR spectra of these cations exhibit in each case a resonance for the gold-bound phosphine ligand and two resonances for the phosphide ligands with very different chemical shifts (ca. 270 and 193 ppm). The more shielded phosphide resonance in each case has a chemical shift comparable to those of the PEt_2 bridges in compounds **1** or **2**, therefore it can be safely assigned to that ligand bridging the molybdenum atoms. Then, the most deshielded resonance must be due to the ligand bridging the Mo and Au atoms. Unfortunately we have found no previous examples of complexes having PR_2 bridges over Mo−Au bonds to check the generality of this deshielding effect. However, we note that complexes having PR_2 ligands bridging M and Au atoms without an M−Au bond have considerably lower chemical shifts.[22] Thus, it seems that the deshielding influence of metal−metal bonds usually observed for the P nuclei of PR_2 bridging ligands[23] also holds for heterometallic Mo−Au bonds.

DFT Studies on the Dicarbonyl Complexes $[Mo_2Cp_2(\mu\text{-}PR_2)_2(CO)_2]$ (R = Cy, Et). As we have seen in the preceding sections, the formation of the gold compounds **1** to **3** is effectively initiated in all cases by the electrophilic attack of the $Au(PR_3)^+$ cation on a Mo−P bond of the neutral diethylphosphide complex $[Mo_2Cp_2(\mu\text{-}PEt_2)_2(CO)_2]$. This is the same conclusion we reached when studying the protonation reactions of this dimolybdenum complex or those of its dicyclohexylphosphide analogue, as stated in the introductory section.[1] To better understand the origin of this rather unexpected result we have carried out DFT[24] calculations on both neutral substrates (see the Experimental Section for details). The electronic structure and bonding in these unsaturated molecules has been analyzed mainly through the properties of the relevant molecular orbitals, but the topological properties of the electron density, as managed in the atoms in molecules (AIM) theory,[25] have been also examined.

Table 4. Selected Data for the DFT-Optimized Geometries of Complexes $[Mo_2Cp_2(\mu\text{-}PR_2)_2(CO)_2]$ (R = Cy, Et)[a]

parameter	R = Cy	R = Et	Exp (R = Ph)[b]
Mo1−Mo2	2.767	2.768	2.713(1)
Mo1−P1	2.448	2.442	2.398(2)
Mo1−P2	2.448	2.435	2.398(2)
Mo2−P1	2.461	2.440	2.398(2)
Mo2−P2	2.461	2.433	2.398(2)
Mo1−C1	1.953	1.947	1.943(7)
Mo2−C2	1.939	1.951	1.943(7)
C1−Mo1−Mo2	87.9	77.9	77.4(2)
C2−Mo2−Mo1	75.0	83.5	77.4(2)

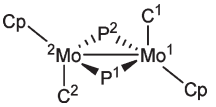

[a] Bond lengths (Å) and angles (deg) according to the labeling shown in the figure. See the Experimental Section for details of the DFT calculations. [b] Averaged figures for the two independent centrosymmetric molecules present in the crystal lattice (see reference 26)

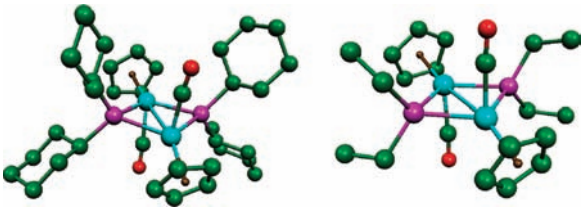

Figure 4. DFT-optimized geometries for compounds $[Mo_2Cp_2(\mu\text{-}PR_2)_2(CO)_2]$ (R = Cy, Et), with H atoms omitted for clarity.

The most relevant parameters derived from the geometry optimization of the compounds $[Mo_2Cp_2(\mu\text{-}PR_2)_2(CO)_2]$ (R = Cy. Et) can be found in the Table 4, with the corresponding views being collected in the Figure 4. The optimized bond lengths are in quite good agreement with the corresponding experimental data in the complex $[Mo_2Cp_2(\mu\text{-}PPh_2)_2(CO)_2]$ as measured using X-ray diffraction,[26] although the computed values for lengths involving the metal atoms tend to be slightly longer (less than 0.05 Å) than the corresponding experimental data. This is a common tendency with the functionals currently used in the DFT computations of transition metal compounds.[24a,27] As expected, a short intermetallic length (ca. 2.77 Å) is computed for both molecules, in agreement with the formal double Mo−Mo to be proposed for these 32-electron complexes under the EAN formalism. Yet these values are longer than the figures recently computed for the isoelectronic carbyne complexes $[Mo_2Cp_2(\mu\text{-}COMe)(\mu\text{-}PCy_2)(CO)_2]$ (2.734 Å) and $[Mo_2Cp_2\{\mu\text{-}C(CO_2Me)\}(\mu\text{-}PCy_2)(CO)_2]$ (2.699 Å),[10] a difference that can be attributed to the bigger size of the P donor atoms, compared to carbon. As usually found for these types of *trans*-dicarbonyl complexes, the carbonyl ligands are slightly bent over the M−M bond, but the bending is quite asymmetric for the dicyclohexylphosphide complex, with one ligand strongly bent over the intermetallic bond (75°) and the other one almost perpendicular to it (87.9°). This distortion seems to be caused by the need of

(22) (a) Blanco, M. C.; Fernández, E. J.; Jones, P. G.; Laguna, A.; López-Luzuriaga, J. M.; Olmos, M. E. *Angew. Chem., Int. Ed.* **1998**, *37*, 3042. (b) Livotto, F. S.; Vargas, M. D.; Braga, D.; Grepioni, F. *J. Chem. Soc., Dalton Trans.* **1992**, 577. (c) Carriedo, G. A.; Riera, V.; Rodriguez, M. L.; Jones, P. G.; Latner, J. *J. Chem. Soc., Dalton Trans.* **1989**, 639.

(23) Carty, A. J.; McLaughin, S. A.; Nucciarone, D. In *Phosphorus-31 NMR Spectroscopy in Stereochemical Analysis*; Verkade, J. G., Quin, L. D., Eds.; VCH: New York, 1987; Chapter 16.

(24) (a) Koch, W.; Holthausen, M. C. *A Chemist's Guide to Density Functional Theory*, 2nd ed.; Wiley-VCH: Weinheim, 2002. (b) Ziegler, T. *Chem. Rev.* **1991**, *91*, 651. (c) Foresman, J. B.; Frisch, ó. *Exploring Chemistry with Electronic Structure Methods*, 2nd ed.; Gaussian, Inc.: Pittsburg, 1996.

(25) (a) Bader, R. F. W. *Atoms in molecules-A Quantum Theory*; Oxford University Press: Oxford, U. K., 1990.

(26) Adatia, T.; McPartlin, M.; Mays, M. J.; Morris, M. J.; Raithby, P. R. *J. Chem. Soc., Dalton Trans.* **1989**, 1555.

(27) Cramer, C. J. *Essentials of Computational Chemistry*, 2nd ed.; Wiley: Chichester, U.K., 2004.

Table 5. Selected Atomic Charges in the Complexes $[Mo_2Cp_2(\mu\text{-}PR_2)_2(CO)_2]$ (R = Cy, Et)[a]

	Mulliken		NPA	
atom	R = Cy	R = Et	R = Cy	R = Et
Mo1	−0.45	−0.32	−0.29	−0.24
Mo2	−0.36	−0.37	−0.19	−0.28
P1	0.53	0.49	0.80	0.78
P2	0.53	0.49	0.80	0.80
C1	0.23	0.27	0.56	0.54
C2	0.27	0.25	0.54	0.55
O1	−0.32	−0.33	−0.51	−0.51
O2	−0.34	−0.32	−0.52	−0.50

[a] Charges according to the labeling shown in the Table 4. See the Experimental Section for details of the DFT calculations.

avoiding unfavorable contacts with one of the Cy rings, and thus suggests that there is significant steric crowding in the dicyclohexyl compound. As stated above, we suspect that the failure of this substrate to react with $Au(PR_3)^+$ cations might in fact have an steric origin.

The atomic charges computed for these dicarbonyl molecules are collected in Table 5, which includes Mulliken charges,[28] and those derived from the NBO analysis (NPA charges).[29] The picture is similar in both complexes under either scheme, with the largest negative charges being located at the oxygen and metal atoms, whereas the P-donor atoms bear large positive charges. Thus, we could predict that, under conditions of charge control, an electrophile would rather attack either the O(carbonyl) or the metal atoms. This might explain the formation of the hydride intermediates $[M_2Cp_2(H)(\mu\text{-}PR_2)(\mu\text{-}PR'_2)(CO)_2]^+$ (observed when M = W, and also when M = Mo and R = R′ = Ph) in our previous protonation studies[1] but obviously cannot account for the formation of agostic complexes of type $[Mo_2Cp_2(\mu\text{-}\kappa^2\text{-}HPR_2)(\mu\text{-}PR'_2)(CO)_2]^+$ nor the agostic-like complexes **1**. The latter species must follow from suitable orbital interactions.

A detailed study of the molecular orbital diagrams for edge-sharing bioctahedral complexes was reported early on by Hoffmann and co-workers,[30] and was revisited and widened recently by Alvarez and co-workers.[31] The metal−metal bonding in these systems follows from the occupation of one σ, one π, and one δ bonding MOs, with their corresponding antibonding combinations being the next ones in energy. Using this scheme as a first approach, we might therefore expect a frontier configuration of the type $\sigma^2\pi^2\delta^2(\delta^*)^2$ for the 32-electron complexes $[Mo_2Cp_2(\mu\text{-}PR_2)_2(CO)_2]$, are thus a double metal−metal bond, in agreement with the EAN formalism. This situation, however, can be significantly modified in each particular complex as a result of orbital mixing, especially when π-acceptor ligands are present.

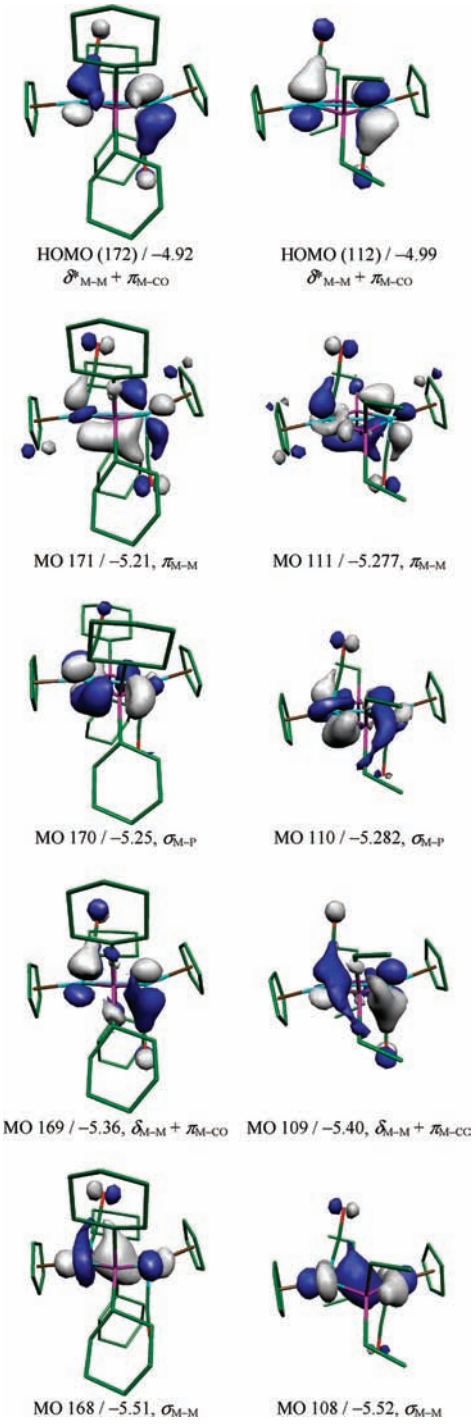

Figure 5. Selected molecular orbitals of complexes $[Mo_2Cp_2(\mu\text{-}PR_2)_2(CO)_2]$ (R = Cy, Et), with their energies and main bonding character indicated below.

The most relevant molecular orbitals of compounds $[Mo_2Cp_2(\mu\text{-}PR_2)_2(CO)_2]$ (R = Cy, Et) are depicted in the Figure 5, along with their associated energy and prevalent bonding character. As predicted, the HOMO has a metal−metal antibonding δ^* character, although it also has a significant metal to carbonyl $\pi_{M\text{-}CO}$ backbonding contribution. Not far below in energy there is a group of four orbitals, three of them accounting for the expected metal−metal bonding interactions (with π, δ, and σ characters, in order of decreasing energy). Thus, the double

(28) Mulliken, R. S. *J. Chem. Phys.* **1955**, *23*, 1833.
(29) Mulliken population analysis fails to give a useful and reliable characterization of the charge distribution in many cases, especially when highly ionic compounds and diffuse basis functions are involved. Charges calculated according to the natural population analysis (NPA) do not show these deficiencies and are more independent of the basis set(a) Reed, A. E.; Weinstock, R. B.; Weinhold, F. *J. Chem. Phys.* **1985**, *83*, 735. (b) Reed, A. E.; Curtis, L. A.; Weinhold, F. *Chem. Rev.* **1988**, *88*, 899.
(30) Shaik, S.; Hoffmann, R.; Fiessel, C. R.; Summerville, R. H. *J. Am. Chem. Soc.* **1980**, *102*, 4555.
(31) Palacios, A. A.; Aullón, G.; Alemany, P.; Alvarez, S. *Inorg. Chem.* **2000**, *39*, 3166.

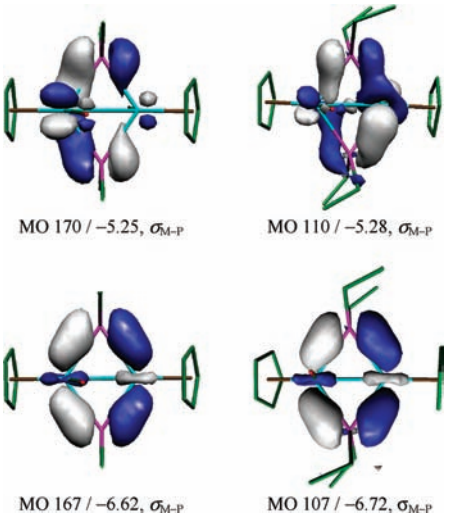

Figure 6. High-energy framework molecular orbitals of complexes $[Mo_2Cp_2(\mu\text{-}PR_2)_2(CO)_2]$ (R = Cy, Et), as viewed from above the Mo_2P_2 framework, with their energies and main bonding character indicated below. The Cy rings (except the C^1 atoms) have been omitted for clarity.

metal−metal bond in these compounds can be properly described as having σ and π components, as anticipated. However, the fourth orbital within this group (HOMO−2), energetically placed between the δ and π components of the intermetallic bonding, does not represent a metal−metal interaction, but instead corresponds to one of the four molecular orbitals accounting for the M−P bonding in the flat Mo_2P_2 framework. Pictures of this orbital for both computed molecules, as viewed from above the Mo_2P_2 plane, are shown in the Figure 6.

The above frontier orbitals are critical to the understanding of the different products observed in the reactions of the phosphide complexes of type $[M_2Cp_2(\mu\text{-}PR_2)(\mu\text{-}PR'_2)(CO)_2]$ with H^+ or $Au(PR_3)^+$ cations. Thus, since the highest occupied molecular orbital (HOMO) in these complexes represents electron density mostly concentrated at the metal atoms, with the more prominent lobes close to the carbonyl ligands, it has the right shape to account for a terminal attachment of the incoming electrophile, which is also favored under electrostatic grounds as stated above, thus explaining the formation of hydride intermediates of the type $[M_2Cp_2(H)(\mu\text{-}PR_2)(\mu\text{-}PR'_2)(CO)_2]^+$, where the terminal hydride ligand is placed *cis* to a carbonyl ligand.[1] The interaction of an electrophile with the HOMO−1 might be considered yet as another likely event, also favored on electrostatic grounds. This would imply the attachment of the incoming electrophile to the metal−metal bond, but such a process has not been observed by us in any instance. To justify this, we can guess that the approach of an electrophile from above the M_2P_2 plane might lead to unfavorable repulsions with the substituents at the P atoms and even with the carbonyl ligands, since the latter are bent over the metal−metal bond and thus should act effectively as a barrier for such an approach.

The interaction of an incoming electrophile with the HOMO−2 orbital, finally, has the right shape to explain the formation of the agostic complexes of type $[Mo_2Cp_2(\mu\text{-}\kappa^2\text{-}HPR_2)(\mu\text{-}PR'_2)(CO)_2]^+$ or the agostic-type gold complexes **1a,b**, since the more prominent lobes of this Mo−P bonding orbital are directed slightly above or below the Mo_2P_2 plane and opposite the nearest carbonyl. This is in contrast to the interaction arising from the HOMO, expected to occur close to the carbonyl ligands as discussed above. Therefore, we could anticipate that the interaction between a generic electrophile with the HOMO−2 might be more favored on steric grounds, when compared to an interaction with the HOMO. The presence of this M−P bonding orbital within the group of frontier orbitals in our diphosphide complexes is somewhat unexpected, since this type of framework orbitals are usually found well below the metal-only orbitals. This is the case of the next framework orbital (HOMO−5, that is, MO167 and MO107, respectively), which is placed more than 1 eV below the corresponding σ_{MM} orbital, as expected (Figure 6). However, we note that Extended-Hückel calculations carried out previously to determine the influence of the mutual approach of the metal fragments (as defined by the X−M−X angle) on the energy of the framework bonding orbitals in complexes of the type $[M_2(\mu\text{-}XR_2)_2L_8]$ predicted for the orbital analogous to our HOMO−2 a rise in energy of about 2 eV upon opening of the XMX angle from about 75° up to 120°.[31] In the case of our PR_2-bridged complexes, the computed P−Mo−P angles are 112.2° (R = Cy) and 110.8° (R = Et) and thus can explain at least in part the unusually high energy of the centrosymmetric framework orbital. This effect is surely reinforced by the presence of electron-donor substituents at the P atoms, a factor that in our previous protonation studies was experimentally found to favor the thermodynamic stability of agostic complexes of the type $[Mo_2Cp_2(\mu\text{-}\kappa^2\text{-}HPR_2)(\mu\text{-}PR'_2)(CO)_2]^+$.[1] In any case, we should conclude that the attack of a generic electrophile on the M−P bonds of our diphosphide complexes, as required to form the observed agostic and agostic-like products, is derived indirectly from the unsaturated nature of these 32-electron substrates, since the close intermetallic approach imposed by the multiple metal−metal binding has a destabilizing effect on the framework Mo−P bonds, thus enabling the corresponding electrons to be involved in donor−acceptor interactions with external electrophiles.

Reaction of the Complex $[Mo_2Cp_2(\mu\text{-}COMe)(\mu\text{-}PCy_2)(CO)_2]$ with $[Au\{P(p\text{-}tol)_3\}]^+$. The structure and bonding in the diphosphide complexes $[Mo_2Cp_2(\mu\text{-}PR_2)_2(CO)_2]$ just discussed is completely analogous to that recently computed for the 32-electron methoxycarbyne complex $[Mo_2Cp_2(\mu\text{-}COMe)(\mu\text{-}PCy_2)(CO)_2]$.[10] The double metal−metal bond in the latter molecule is derived from a frontier configuration now of the type $\delta^2\sigma^2\pi^2(\delta^*)^2$ and is also characterized by a high electron density of about 0.42 e $Å^{-3}$ at the Mo−Mo bond critical point, to be compared with values of about 0.41 e $Å^{-3}$ in our diphosphide complexes (see Supporting Information). Interestingly, the carbyne complex also exhibits a high-energy framework bonding orbital, it actually being the HOMO−1 and having both Mo−P and Mo−C(carbyne) bonding character. Thus it was of interest to examine if this complex could add gold(I) electrophiles to give agostic-type or carbyne-bridged derivatives, depending on whether the electrophilic attack were to occur at either the Mo−P or the Mo−C bonds.

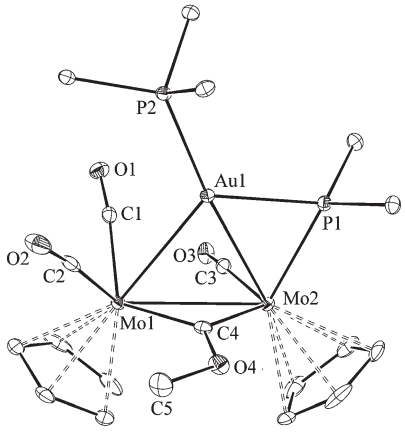

Figure 7. ORTEP diagram (30% probability) of the cation in compound **4**, with H atoms, Cy groups (except the C^1 atoms), and *p*-tol groups (except the C^1 atoms) omitted for clarity.

Table 6. Selected Bond Lengths (Å) and Angles (deg) for Compound **4**

Mo(1)−Mo(2)	2.987(1)	Mo(1)−Au(1)−Mo(2)	64.0(1)
Mo(1)−Au(1)	2.864(1)	Au(1)−P(1)−Mo(2)	71.5(1)
Mo(2)−Au(1)	2.769(1)	Mo(1)−C(4)−Mo(2)	93.6(1)
Mo(1)−C(4)	2.055(3)	C(4)−O(4)−C(5)	120.5(3)
Mo(2)−C(4)	2.041(3)	Mo(1)−Mo(2)−C(3)	71.3(1)
Au(1)−C(4)	2.530(3)	Mo(2)−Mo(1)−C(1)	93.0(1)
Mo(2)−P(1)	2.364(1)	Mo(2)−Mo(1)−C(2)	121.8(2)
Au(1)−P(1)	2.373(1)	P(1)−Mo(2)−C(3)	96.8(1)
Mo(1)−C(1)	2.017(3)	P(1)−Mo(2)−C(4)	103.5(1)
Mo(1)−C(2)	1.977(4)	P(2)−Au(1)−Mo(2)	174.6(1)
Mo(2)−C(3)	1.967(3)	P(2)−Au(1)−Mo(1)	121.25(2)
Au(1)−C(1)	2.741(3)	P(2)−Au(1)−P (1)	120.82(3)
C(4)−O(4)	1.322(4)	Au(1)−Mo(2)−C(3)	84.7(1)
O(4)−C(5)	1.453(4)	Mo(1)−C(1)−O(1)	172.8(3)
		Mo(1)−C(2)−O(2)	174.6(3)
		Mo(2)−C(3)−O(3)	167.5(3)

When a freshly prepared solution of [Au{P(*p*-tol)$_3$}(THT)]PF_6 in THF is mixed with the above carbyne complex, an orange solution containing a mixture of products is rapidly formed. Upon chromatographic workup of this mixture, the tricarbonyl cluster [$Au{Mo_2}(\mu$-COMe)(μ-PCy_2)$(CO)_3${P(*p*-tol)$_3$}]PF_6 (**4**) could be isolated in moderate yield (Chart 1). Unfortunately, attempts to increase the selectivity of this reaction by modifying the reaction conditions (temperature, solvent, and method of generating the gold(I) electrophile) were unsuccessful.

The structure of compound **4** has been confirmed through an X-ray diffraction study, and it is shown in the Figure 7, while the most relevant bond distances and angles are collected in the Table 6. The molecule is very similar to that found for **3b**, after replacing the phosphide ligand bridging the molybdenum atoms by a rather symmetrical methoxycarbyne group displaying Mo−C lengths (ca. 2.05 A) comparable to other methoxycarbyne-bridged Mo_2 and W_2 complexes previously reported by us.[19,32] There are two significant differences, however, with respect to the structure of the diphosphide cluster **3b**: (a) the MoCp(CO) fragments in **4** are arranged in a cisoid conformation and (b) there are no significant semibridging interactions of the carbonyl ligands with the gold atom, with the closest approach being Au(1)−C(1) = 2.741(3) Å. Other structural features in **4** are comparable to those discussed for **3b** and therefore deserve no further comments. We note, however, that the unusual environment around the gold atom now can be considered closer to planar trigonal, rather than T-shaped, with P(2)−Au(1)−Q, P(2)−Au(1)−P(1), and Q−Au(1)−P(1) angles of about 153, 121, and 87° (Q = centroid of the Mo−Mo vector), perhaps as a result of the higher steric demands imposed by the bulkier (compared to PEt_2) PCy_2 ligand, which is placed in the intermetallic plane, as it is the phosphine ligand.

The spectroscopic data for compound **4** in solution (Table 2 and Experimental Section) are fully consistent with its solid-state structure. The IR spectrum exhibits three C−O stretching bands with frequencies higher than those of the diphosphide complex **3a**, in agreement with the better acceptor properties of the methoxycarbyne ligand and with the absence of any semibridging interaction of the carbonyls. We note that the relative intensities of these bands are also different from those of compounds **3**, a feature consistent with the distinct relative arrangements of the Mo(CO) and $Mo(CO)_2$ fragments in the solid state for both species. The unique phosphide ligand bridging the Mo−Au edge gives rise to a quite deshielded ^{31}P NMR resonance (286.3 ppm), in a position comparable to the most deshielded resonance in compounds **3** (ca. 270 ppm). Finally, the methoxycarbyne ligand gives rise also to a strongly deshielded ^{13}C NMR resonance (δ_C = 379.9 ppm), not much more shielded than that of its binuclear precursor (δ_C = 404.0 ppm),[12] in agreement with the retention of the edge-bridging (μ_2) coordination mode of this ligand.

Although we have not been able to characterize the intermediate species preceding the formation of the tricarbonyl cluster **4**, the structural relationship between this compound and the diphosphide clusters **3a,b** makes reasonable the assumption that these reactions proceed analogously (Scheme 4). Thus, we trust that the gold(I) cation most probably attacks selectively the Mo−P bond

Scheme 4. Reaction Pathway Proposed for the Addition of the [Au{P(*p*-tol)$_3$}]$^+$ Cation to the Carbyne Complex [$Mo_2Cp_2(\mu$-COMe)(μ-PCy_2)$(CO)_2$]

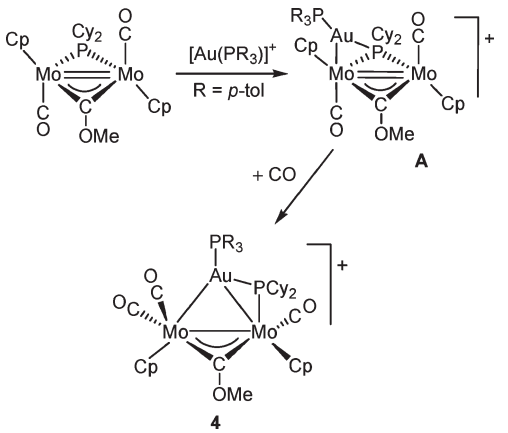

(32) (a) Alvarez, C. M.; Alvarez, M. A.; García, M. E.; García-Vivó, D.; Ruiz, M. A. *Organometallics* **2005**, *24*, 4122. (b) García, M. E.; Melón, S.; Ramos, A.; Riera, V.; Ruiz, M. A.; Belleti, D.; Graiff, C.; Tiripicchio, A. *Organometallics* **2003**, *22*, 1983. (c) García, M. E.; Riera, V.; Rueda, M. T.; Ruiz, M. A. *J. Am. Chem. Soc.* **1999**, *121*, 1960.

of the carbyne substrate (interaction with the corresponding HOMO-1 frontier orbital) to give an agostic-like intermediate **A** analogous to the diphosphide complexes **1**. That intermediate would be quite unstable and it would rapidly decompose, then liberating carbon monoxide that would add to other molecules of **A** to give the electron-precise tricarbonyl **4** finally isolated. The transformation **A**/**4** is completely analogous to the transformations **1**/**3** discussed above (the latter, however, taking place slowly in the absence of added CO), and implies the displacement of the μ_3-PR_2 ligand to a more usual μ_2-coordination mode. By virtue of the isolobal analogies, the tricarbonyl cations **3** and **4** might be related to a hypothetical phosphine cation with an agostic P−H interaction halfway to be destroyed as a result of the carbonylation on an agostic unsaturated cation of the type $[Mo_2Cp_2(\mu\text{-}\kappa^2\text{-}HPR_2)(\mu\text{-}X)(CO)_2]^+$. Though an interesting comparison, we must note that the actual reaction of the dicyclohexylphosphide cation $[Mo_2Cp_2(\mu\text{-}\kappa^2\text{-}HPCy_2)(\mu\text{-}PCy_2)(CO)_2]^+$ with CO does not takes place at room temperature and atmospheric pressure, while the reaction with CN^{t}Bu does not result in the simple addition of the ligand, but also in the replacement of CO, this triggering the oxidative addition (rather than detachment) of the agostic P−H bond.[1]

Concluding Remarks

The reactions of the diphosphide complex $[Mo_2Cp_2(\mu\text{-}PEt_2)_2(CO)_2]$ with the gold(I) cations $[Au(PR_3)]^+$ (R = *p*-tol, Me) proceed analogously to the protonation reactions and are initiated through the binding of the incoming electrophile to one of the Mo−P bonds of the neutral substrate and *trans* to the closest carbonyl ligand, to give an agostic-like cation $[AuMo_2Cp_2(\mu\text{-}PEt_2)(\mu_3\text{-}PEt_2)(CO)_2(PR_3)]^+$. This kinetic product then partially rearranges to reach an equilibrium with the corresponding hydride-like isomer $[AuMo_2Cp_2(\mu\text{-}PEt_2)_2(CO)_2(PR_3)]^+$. All these unsaturated cations react with CO to give the electron-precise derivatives $[AuMo_2Cp_2(\mu\text{-}PEt_2)_2(CO)_3(PR_3)]^+$, this implying the rearrangement of the μ_3-PEt_2 ligand into a more common μ_2-coordination mode. According to our DFT calculations, we conclude that the formation of agostic and agostic-like products in the reactions of the dimolybdenum complexes $[Mo_2Cp_2(\mu\text{-}PR_2)_2(CO)_2]$ (R = Cy, Et) with H^+ and $[Au(PR_3)]^+$ cations is an orbital-controlled process made possible by the presence in these neutral substrates of a framework M−P bonding orbital high in energy. Such unusual circumstance is an indirect consequence of the multiple intermetallic bonding in these substrates, since the latter imposes a close approach of the metal centers, which in turn increases the energy of the framework orbitals. The carbyne complex $[Mo_2Cp_2(\mu\text{-}COMe)(\mu\text{-}PCy_2)(CO)_2]$ also has a high-energy framework orbital with M−P and M−C bonding character, and thus potentially could behave similarly when reacting with gold(I) cations. Indeed, the reaction with $[Au\{P(p\text{-}tol)_3\}]^+$ to give the tricarbonyl $[AuMo_2Cp_2(\mu\text{-}COMe)(\mu\text{-}PCy_2)(CO)_3\{P(p\text{-}tol)_3\}]^+$ suggests that this is the case, with this reaction most likely being initiated by the binding of the gold cation to one of the Mo−P bonds of the carbyne complex.

Experimental Section

General Procedures and Starting Materials. All manipulations and reactions were carried out under a nitrogen (99.995%) atmosphere using standard Schlenk techniques. Solvents were purified according to literature procedures and distilled prior to use.[33] Petroleum ether refers to that fraction distilling in the range 338−343 K. The compounds $[Mo_2Cp_2(\mu\text{-}PEt)_2(CO)_2]$,[5] $[Mo_2Cp_2(\mu\text{-}COMe)(\mu\text{-}PCy_2)(CO)_2]$,[10] and $[AuCl(PR_3)]$ [R = (*p*-tol), Me][34] were prepared as described previously. Chromatographic separations were carried out using jacketed columns cooled by tap water (ca. 288 K). Commercial aluminum oxide (Aldrich, activity I, 150 mesh) was degassed under vacuum prior to use. The latter was mixed under nitrogen with the appropriate amount of water to reach the activity desired. All other reagents were obtained from the usual commercial suppliers and used as received. IR stretching frequencies were measured in solution or Nujol mulls and are referred to as ν (solvent) or ν (Nujol) respectively. Nuclear Magnetic Resonance (NMR) spectra were routinely recorded at 300.09 (^{1}H), 121.50 (^{31}P{^{1}H}), or 75.47 MHz (^{13}C{^{1}H}) at 290 K in CD_2Cl_2 solutions unless otherwise stated. Chemical shifts (δ) are given in parts per million, relative to internal tetramethylsilane (^{1}H, ^{13}C) or external 85% aqueous H_3PO_4 (^{31}P). Coupling constants (J) are given in hertz.

Preparation of Compounds $[AuMo_2Cp_2(\mu\text{-}PEt_2)(\mu_3\text{-}PEt_2)(CO)_2\{P(p\text{-}tol)_3\}]PF_6$ (1a) and $[AuMo_2Cp_2(\mu\text{-}PEt_2)_2(CO)_2\{P(p\text{-}tol)_3\}]PF_6$ (2a). A green solution of compound $[Mo_2Cp_2(\mu\text{-}PEt_2)_2(CO)_2]$ (0.030 g, 0.056 mmol) in dichloromethane (5 mL) was stirred with $[AuCl\{P(p\text{-}tol)_3\}]$ (0.042 g, 0.078 mmol) and $TlPF_6$ (0.030 g, 0.086 mmol) for 6 h to give a brown suspension which was filtered using a canula. The resulting orange solution was shown (by NMR) to contain an equilibrium mixture of compounds **1a** and **2a** in a ratio 1:3, along with some side-products (gold complexes). The solvent was then removed under vacuum, and the residue was washed with petroleum ether (3 × 5 mL) and crystallized from dichloromethane-petroleum ether to give an orange powder (0.035 g, 52%). The crystals of compound **2a** used in the X-ray study were grown by the slow diffusion of toluene into a THF solution of the complex at 253 K. Anal. Calcd for $C_{45}H_{59}AuF_6Mo_2O_3P_4$ (**2a**·THF): C, 42.40; H, 4.66. Found: C, 42.19; H, 4.58. *Spectroscopic data for* ***1a****:* ^{1}H NMR: δ 7.44−6.91 (m, 12H, C_6H_4), 5.64, 5.37 (2*s*, 2 × 5H, Cp), 3.36, 3.25, 2.95, 2.72 (4*m*, 4 × 1H, CH_2), 2.43 (s, 9H, C_6H_4−CH_3), 2.10, 1.87 (2*m*, 2 × 2H, CH_2), 1.65−0.71 (m, 12H, CH_3). *Spectroscopic data for* ***2a****:* ^{1}H NMR: δ 7.44−6.91 (m, 12H, C_6H_4), 5.22 (s, 10H, Cp), 2.84 (m, 4H, CH_2), 2.41 (s, 9H, C_6H_4−CH_3), 2.31 (m, 4H, CH_2), 1.65−0.71 (m, 12H, CH_3).

Reaction with the Cation $[Au(PMe_3)]^+$. A solution of $[Mo_2Cp_2(\mu\text{-}PEt_2)_2(CO)_2]$ (0.025 g, 0.047 mmol) in dichloromethane (5 mL) was stirred at 273 K with $[AuCl(PMe_3)]$ (0.024 g, 0.077 mmol) and $TlPF_6$ (0.030 g, 0.086 mmol) for 24 h to give an orange suspension which was filtered using a canula. The resulting orange solution was shown (by NMR) to be an equilibrium mixture of compounds $[AuMo_2Cp_2(\mu\text{-}PEt_2)(\mu_3\text{-}PEt_2)(CO)_2(PMe_3)]PF_6$ (**1b**) and $[AuMo_2Cp_2(\mu\text{-}PEt_2)_2(CO)_2(PMe_3)]PF_6$ (**2b**) in an equimolar ratio, along with some side-products (gold complexes) and a small amount of the tricarbonyl compound **3b**. The solvent was then removed under vacuum, and the residue was washed with petroleum ether (3 × 5 mL) to give an impure orange powder which could not be properly purified through crystallization because of its progressive decomposition. *Spectroscopic data for* ***1b****:* ^{1}H NMR (400.13 MHz): δ 5.78, 5.47 (2*s*, 2 × 5H, Cp), 3.35 (m, 4H, 2 × CH_2), 2.18, 2.13 (2*m*, 2 × 2H, CH_2), 1.94−0.88 (m, 21H, CH_3). *Spectroscopic data for* ***2b****:* ^{1}H NMR (400.09 MHz): δ 5.26 (s,

(33) Armarego, W. L. F.; Chai, C. *Purification of Laboratory Chemicals*, 5th ed.; Butterworth-Heinemann: Oxford, U.K., 2003.
(34) Braunstein, P.; Lehrer, H.; Matt, D. *Inorg. Synth.* **1990**, 218.

10H, Cp), 2.76 (m, 4H, CH_2), 2.30 (m, 4H, CH_2), 1.94−0.88 (m, 21H, CH_3).

Preparation of [AuMo$_2$Cp$_2$(μ-PEt$_2$)$_2$(CO)$_3${P(*p*-tol)$_3$}]PF$_6$ (3a). An equilibrium mixture of isomers **1a** and **2a** (0.070 g, 0.058 mmol) in dichloromethane (5 mL) was stirred at room temperature under an atmosphere of carbon monoxide for 16 h to give an orange solution. The solvent was then removed from the mixture under vacuum, and the residue was dissolved in a minimum dichloromethane and chromatographed through an alumina column (activity IV) at 288 K. Elution with dichloromethane gave an orange fraction yielding, after removal of solvents under vacuum, compound **3a** as an orange microcrystalline solid (0.045 g, 63%). Anal. Calcd for $C_{42}H_{51}AuF_6Mo_2O_3P_4$: C, 40.99; H, 4.18. Found: C, 41.06; H, 4.12. ^{1}H NMR: δ 7.44−6.91 (m, 12H, C_6H_4), 5.64, 5.37 (2*s*, 2 × 5H, Cp), 3.25 (m, 2H, CH_2), 2.70 (m, 4H, CH_2), 2.43 (s, 9H, C_6H_4−CH_3), 1.87 (m, 2H, CH_2), 1.65−0.71 (m, 12H, CH_3).

Preparation of [AuMo$_2$Cp$_2$(μ-PEt$_2$)$_2$(CO)$_3$(PMe$_3$)]PF$_6$ (3b). An equilibrium mixture of isomers **1b** and **2b** was prepared in situ starting from [Mo$_2$Cp$_2$(μ-PEt$_2$)$_2$(CO)$_2$] (0.030 g, 0.056 mmol) in dichloromethane (5 mL) as described above, and this mixture was further stirred for 2 h at room temperature under an atmosphere of carbon monoxide to give an orange solution. The solvent was then removed from the mixture under vacuum, and the residue was dissolved in a minimum of dichloromethane and chromatographed through an alumina column (activity IV) at 288 K. Elution with dichloromethane yielded an orange fraction. Removal of solvents under vacuum from the latter fraction gave compound **3b** as an orange microcrystalline solid (0.035 g, 75%). The crystals used in the X-ray study were grown by the slow diffusion of a layer of petroleum ether into a dichloromethane solution of the complex at 253 K. Anal. Calcd for $C_{24}H_{39}AuF_6Mo_2O_3P_4$: C, 28.76; H, 3.92. Found: C, 28.57; H, 3.80. ^{1}H NMR (400.13 MHz): δ 5.40, 5.19 (2*s*, 2 × 5H, Cp), 3.14, 2.97, 2.53, 2.42 (4*m*, 4 × 2H, CH_2), 1.83−1.08 (m, 21H, CH_3).

Preparation of [AuMo$_2$Cp$_2$(μ-COMe)(μ-PCy$_2$)(CO)$_3$(PMe$_3$)]PF$_6$ (4). A THF solution (10 mL) of [Au{P(*p*-tol)$_3$}(THT)]PF$_6$ was prepared in situ by stirring [AuCl{P(*p*-tol)$_3$}] (0.027 g, 0.050 mmol) and TlPF$_6$ (0.017 g, 0.048 mmol) in the presence of THT (tetrahydrothiophen, 0.1 mL, excess) for 10 min. The solution was filtered using a canula and then added to compound [Mo$_2$Cp$_2$(μ-COMe)(μ-PCy$_2$)(CO)$_2$] (0.030 g, 0.048 mmol) to give an orange solution instantaneously. Solvent was then removed under vacuum, the residue was extracted with dichloromethane-petroleum ether (1:1), and the extract was chromatographed through alumina (activity IV) at 288 K. Elution with dichloromethane gave an orange fraction which yielded, after removal of solvents under vacuum, compound **4** as an orange microcrystalline solid (0.029 g, 46%). The crystals used in the X-ray study were grown by the slow diffusion of a layer of petroleum ether into a dichloromethane solution of the complex at 253 K. Anal. Calcd for $C_{48}H_{56}AuF_6Mo_2O_4P_3$: C, 44.60; H, 4.37. Found: C, 44.46; H, 4.21. ^{1}H NMR: δ 7.26 [dd, J_{PH} = 2, J_{HH} = 8, 6H, H^3(C_6H_4)], 7.12 [dd, J_{HH} = 8, J_{PH} = 12, 6H, H^2(C_6H_4)], 5.30, 5.26 (2*s*, 2 × 5H, Cp), 4.29 (s, 3H, OCH_3), 2.41 (s, 9H, C_6H_4−CH_3), 1.90−0.20 (m, 22H, Cy). ^{13}C{^{1}H} NMR: δ 379.9 (s, μ-COMe), 242.1 (s, br, CO), 223.6 (t, J_{CP} = 5, CO), 223.3 (d, J_{CP} = 2, CO), 142.8 [d, J_{CP} = 4, C^4(C_6H_4)], 133.7 [d, J_{CP} = 13, C^2(C_6H_4)], 130.2 [d, J_{CP} = 11, C^3(C_6H_4)], 127.3 [d, J_{CP} = 52, C^1(C_6H_4)], 90.9, 90.3 (2*s*, Cp), 72.8 (s, OMe), 46.6 [d, J_{CP} = 9, C^1(Cy)], 43.8 [d, J_{CP} = 12, C^1(Cy)], 33.2, 32.9, 32.1, 31.4 [4*s*, C^2(Cy)], 27.6 [d, J_{CP} = 10, C^3(Cy)], 27.6 [d, J_{CP} = 13, C^3(Cy)], 27.2 [d, J_{CP} = 14, C^3(Cy)], 27.0 [d, J_{CP} = 11, C^3(Cy)], 26.2, 25.8 [2*s*, C^4(Cy)], 21.6 (s, Me).

Computational Details. All computations described in this work were carried out using the GAUSSIAN03 package,[35] in which the hybrid method B3LYP was applied with the Becke three parameters exchange functional[36] and the Lee−Yang−Parr correlation functional.[37] Effective core potentials (ECP) and their associated double-ζ LANL2DZ basis set were used for the molybdenum atoms.[38] The light elements (P, O, C, and H) were described with the 6-31G* basis.[39] Geometry optimizations were performed under no symmetry restrictions, using initial coordinates derived from X-ray data of comparable complexes, and frequency analyses were performed to ensure that a minimum structure with no imaginary frequencies was achieved in each case. For interpretation purposes, natural population analysis (NPA) charges[29b] were derived from the natural bond order (NBO) analysis of the data.[29b] Molecular orbitals and vibrational modes were visualized using the Molekel program.[40] The topological analysis of ρ was carried out with the Xaim routine.[41]

X-ray Structure Determination of Compounds 2a, 3b, and 4. The X-ray intensity data were collected on Kappa-Appex-II (**2a**) and Smart-CCD-1000 (**3b**, **4**) Bruker diffractometers using graphite-monochromated Mo Kα radiation. The software APEX[42] was used for collecting frames with the ω/φ scans measurement method for **2a**, and the software SMART[43] was used in the case of **3b** and **4**. The collected frames were then processed for integration by the software SAINT,[43] and a multiscan absorption correction was applied with SADABS.[44] Using the program suite WinGX,[45] the structure was solved by Patterson interpretation and phase expansion, and refined with full-matrix least-squares on F^2 with SHELXL97.[46] All non-hydrogen atoms were refined anisotropically. All hydrogen atoms were geometrically located, and they were given an overall isotropic thermal parameter. The final refinement on F^2 proceeded by full-matrix least-squares calculations. Compound **2a** crystallized with a molecule of THF. In the case of compound **3b** one cyclopentadienyl ligand was found to be disordered in two positions, and was satisfactorily modeled with occupancy factors of 0.60 and 0.40. Besides this, both ethyl groups on P(2) were also disordered over two positions, but a satisfactory modeling of the disorder was not achieved in this case and some

(35) Frisch, M. J.; Trucks, G. W.; Schlegel, H. B.; Scuseria, G. E.; Robb, M. A.; Cheeseman, J. R.; Montgomery, Jr., J. A.; Vreven, T.; Kudin, K. N.; Burant, J. C.; Millam, J. M.; Iyengar, S. S.; Tomasi, J.; Barone, V.; Mennucci, B.; Cossi, M.; Scalmani, G.; Rega, N.; Petersson, G. A.; Nakatsuji, H.; Hada, M.; Ehara, M.; Toyota, K.; Fukuda, R.; Hasegawa, J.; Ishida, M.; Nakajima, T.; Honda, Y.; Kitao, O.; Nakai, H.; Klene, M.; Li, X.; Knox, J. E.; Hratchian, H. P.; Cross, J. B.; Bakken, V.; Adamo, C.; Jaramillo, J.; Gomperts, R.; Stratmann, R. E.; Yazyev, O.; Austin, A. J.; Cammi, R.; Pomelli, C.; Ochterski, J. W.; Ayala, P. Y.; Morokuma, K.; Voth, G. A.; Salvador, P.; Dannenberg, J. J.; Zakrzewski, V. G.; Dapprich, S.; Daniels, A. D.; Strain, M. C.; Farkas, O.; Malick, D. K.; Rabuck, A. D.; Raghavachari, K.; Foresman, J. B.; Ortiz, J. V.; Cui, Q.; Baboul, A. G.; Clifford, S.; Cioslowski, J.; Stefanov, B. B.; Liu, G.; Liashenko, A.; Piskorz, P.; Komaromi, I.; Martin, R. L.; Fox, D. J.; Keith, T.; Al-Laham, M. A.; Peng, C. Y.; Nanayakkara, A.; Challacombe, M.; Gill, P. M. W.; Johnson, B.; Chen, W.; Wong, M. W.; Gonzalez, C.; and Pople, J. A. *Gaussian 03*, Revision B.02; Gaussian, Inc.: Wallingford, CT, 2004.

(36) Becke, A. D. *J. Chem. Phys.* **1993**, *98*, 5648.
(37) Lee, C.; Yang, W.; Parr, R. G. *Phys. Rev. B* **1988**, *37*, 785.
(38) Hay, P. J.; Wadt, W. R. *J. Chem. Phys.* **1985**, *82*, 299.
(39) (a) Hariharan, P. C.; Pople, J. A. *Theor. Chim. Acta* **1973**, *28*, 213. (b) Petersson, G. A.; Al-Laham, M. A. *J. Chem. Phys.* **1991**, *94*, 6081. (c) Petersson, G. A.; Bennett, A.; Tensfeldt, T. G.; Al-Laham, M. A.; Shirley, W. A.; Mantzaris, J. *J. Chem. Phys.* **1988**, *89*, 2193.
(40) Portmann, S.; Lüthi, H. P.; MOLEKEL: An Interactive Molecular Graphics Tool. *Chimia* **2000**, *54*, 766.
(41) Ortiz, J. C.; Bo, C. *Xaim*; Departamento de Química Física e Inorgánica, Universidad Rovira i Virgili: Tarragona, Spain, 1998.
(42) *APEX 2*, version 2.0-1; Bruker AXS Inc: Madison, WI, 2005.
(43) *SMART & SAINT Software Reference Manuals, Version 5.051* (*Windows NT Version*); Bruker Analytical X-ray Instruments: Madison, WI, 1998.
(44) Sheldrick, G. M. *SADABS, Program for Empirical Absorption Correction*; University of Göttingen: Göttingen, Germany, 1996.
(45) Farrugia, L. J. *J. Appl. Crystallogr.* **1999**, *32*, 837.
(46) Sheldrick, G. M. *Acta Crystallogr., Sect. A* **2008**, *64*, 112.

Table 7. Crystal Data for Compounds **2a**, **3b**, and **4**

	2a·THF	**3b**	**4**
mol formula	$C_{45}H_{59}AuF_6Mo_2O_3P_4$	$C_{24}H_{39}AuF_6Mo_2O_3P_4$	$C_{48}H_{56}AuF_6Mo_2O_4P_3$
mol wt	1274.65	1002.28	1292.69
cryst syst	monoclinic	monoclinic	triclinic
space group	$P2_1/n$	$P2_1/n$	$P\bar{1}$
radiation (λ, Å)	0.71073	0.71073	0.71073
a, Å	15.1093(3)	11.842(2)	12.874(3)
b, Å	17.9915(4)	10.290(2)	14.631(3)
c, Å	17.4254(3)	26.454(5)	14.810(3)
α, deg	90	90	74.271(3)
β, deg	95.3650(10)	98.835(3)	83.993(3)
γ, deg	90	90	70.763(4)
V, Å^3	4716.15(16)	3185.3(10)	2534.9(9)
Z	4	4	2
calcd density, g cm^{-3}	1.795	2.090	1.694
absorp coeff, mm^{-1}	3.825	5.632	3.531
temperature, K	100.0(2)	120(2)	100.0(1)
θ range (deg)	1.63−30.51	1.79−26.46	2.09−27.48
index ranges (h, k, l)	−21, 21; −25, 25; −24, 24	−14, 14; 0, 12; 0, 33	−16, 16; −17, 18; 0, 19
no. of reflns collected	202978	36473	45229
no. of indep reflns (R_{int})	14294 (0.0435)	6545 (0.0545)	11492 (0.0344)
no. of reflns with $I > 2\sigma(I)$	11943	5499	10038
R indexes	$R_1 = 0.0242$	$R_1 = 0.0290$	$R_1 = 0.0261$
[data with $I > 2\sigma(I)$][a]	w$R_2 = 0.0411$[b]	w$R_2 = 0.0647$[c]	w$R_2 = 0.0607$[d]
R indexes (all data)[a]	$R_1 = 0.0373$	$R_1 = 0.0370$	$R_1 = 0.0335$
	w$R_2 = 0.0440$[b]	w$R_2 = 0.0676$[c]	w$R_2 = 0.0634$[d]
GOF	1.016	1.071	1.061
no. of restraints/parameters	0/557	2/363	0/581
$\Delta\rho$(max., min.), e Å^{-3}	1.052, −0.742	1.551, −1.543	1.800, −0.878

[a] $R = \sum||F_o| - |F_c||/\sum|F_o|$, $wR = [\sum w(|F_o|^2 - |F_c|^2)^2/\sum w|F_o|^2]^{1/2}$, $w = 1/[\sigma^2(F_o^2) + (aP)^2 + bP]$ where $P = (F_o^2 + 2F_c^2)/3$. [b] $a = 0.0166$, $b = 3.2949$. [c] $a = 0.0269$, $b = 7.0389$. [d] $a = 0.0299$, $b = 2.8450$.

restraints had to be applied on the distances P(2)−C(20) and C(20)−C(21). In the case of compound **4**, the strongest residual peaks after convergence (1.800, −0.878 e Å^{-3}) were located around the $[PF_6]^-$ group, indicative of an incipient disorder in this anion, not resolved. Crystallographic data and structure refinement details for compounds **2a**, **3b**, and **4** are collected in Table 7.

Acknowledgment. We thank the MEC of Spain for a grant (to D.G.V.) and financial support (project CTQ2006-01207/BQU) and also the COST Action CM0802 "PhoSciNet".

Supporting Information Available: Tables of selected molecular orbitals and data from the AIM topological analysis for complexes $[Mo_2Cp_2(\mu\text{-}PR_2)_2(CO)_2]$ (R = Et, Cy) in pdf format, and a CIF file containing the crystallographic data for the structural analysis of compounds **2a**, **3b**, and **4**. This material is available free of charge via the Internet at http://pubs.acs.org.